

# Performance Estimation by Varying the Grain Port Alignment Position in a Hybrid Rocket Motor

Gyandeep and Rajiv Kumar\*

Department of Space Engineering and Rocketry, Birla Institute of Technology, Mesra, Ranchi - 835 215, India

\*E-mail: rajiv@bitmesra.ac.in

## ABSTRACT

A Hybrid Rocket Motor (HRM) is a type of chemical rocket propulsion in which the propellants are stored in different physical states. To counter the low regression rate characteristic of HRM different grain configurations with innovative port techniques has been evolved with time. It creates better mixing and combustion of fuel with oxidizer without having any special injector and energetic additives. A similar technique has been used in the present study. The fuel used in the present study is a solid grain made from polyvinyl chloride with di-butyl phthalate in the 50:50 ratios with gaseous oxygen as an oxidizer. In this paper, analyses are made to study the performance of a hybrid rocket motor by varying the axial alignment of the grain port at varying locations along the length. Due to the offset of the fuel port at varying locations, recirculation zone were created that enhanced the pressure in the combustion chamber by around 1-2 bar. The thrust generated was increased in the range of 10 to 25 N. Regression rate as well as efficiency was also observed to be increased with the use of this port alignment techniques.

**Keywords:** Hybrid rocket; Offset port; Regression rate; Combustion efficiency; Pre-post combustion chamber

## 1. INTRODUCTION

The Hybrid Rocket Motor (HRM) came to light during the early 20<sup>th</sup> century. After that much work has been done for enhancing the performance of hybrid rocket motors. The HRM works with the propellant having different physical phases. The HRM is the simplest form of engine that can be designed. The advantage associated with the hybrid rocket motors are a less hazardous system, fewer safety concerns, stop-restart capability, low-cost system, easy storage, and fabrication. The specific impulse of HRM is better than solid rocket motor and the density impulse of HRM is better than liquid rocket motor<sup>1</sup>. Generally, the propellant combination of solid fuel and liquid oxidizer is preferred for the design of this hybrid rocket motor. Since gases require large vessels for storing significant amounts of mass due to their lower density of it and in the case of solid oxidizers they have lower performance than the liquid oxidizer so the liquid phase is preferred. The propellants used in these systems are hydroxyl-terminated poly-butadiene (HTPB), polymers like polyethylene, PVC-DBP, and liquefying paraffin wax as the fuel, and di-nitrogen tetra-oxide ( $N_2O_4$ ), hydrogen peroxide ( $H_2O_2$ ), liquid oxygen (LOX), and nitrous oxide ( $N_2O$ ) as the oxidizer<sup>2</sup>. The combustion process occurs within the boundary layer attached to the surface of the fuel grain forming the diffusion flame. The heat energy derived from the combustion of the propellants is transformed in the form of kinetic energy through a suitable nozzle to provide thrust. The main issue with the HRM is the low regression rate of solid fuel; to counter this problem many techniques have

been used. Those methods are mainly classified into two types: first, changing the fuel characteristics like adding special binders, metal additives etc.<sup>3-5</sup> and second methods involves using an innovative injection technique with different grain and port configurations<sup>6</sup>. Apart from it, few other methods used to increase the performance of a hybrid rocket are the use of protrusion<sup>7-9</sup>, bluff body<sup>10</sup>, swirl injectors<sup>6, 11-12</sup>, and the use of a pre-post combustion chamber<sup>13</sup>.

Tian<sup>13</sup>, *et al.* has reported that the combustion efficiency of segmented grain was increased by 15 % to 10 %. The simulation and its test results also showed that after-section of the grain has higher regression rate. Sakashi, *et al.*<sup>14</sup> studied the effect of concave-convex surface grain in a hybrid rocket and observed that due to the upstream section of grain which was convex in nature, the regression rate increased and due to concave part regression slightly decreased but the overall regression rate increased with or without swirl injector and it was upto 1.7-2.0 times respectively. They also observed combustion oscillations inside the motor due to the Helmholtz resonance. Kearney<sup>15</sup>, *et al.* studied the circumferential ports and multi-port configurations and stated that the grain length can be shortened through the use of circumferential ports but it had not increased the peak specific impulse (Isp) of the hybrid rocket motor. The circumferential port configuration had the smallest L/D (length to diameter) ratio in comparison with other port configurations. Even the thrust was reported to be increased in comparison to single and multiple circular port configurations.

Makle<sup>16</sup>, *et al.* studied the performance parameters of a hybrid rocket engine with a post-combustion chamber and

stated that the extra space given after solid grain enhances the mixing of the unburnt fuel and oxidizer coming through the flow due to recirculation zones. It also provides increased residence time to combust the mixture and which was observed through the increased combustion efficiency.

Mechentel<sup>17</sup>, *et al.* had studied the effect of motor geometry on fuel regression rate, stability, nozzle erosion, and c\* efficiency by introducing pre- and post-combustion chambers of hybrid rocket motor. They also attempted to scrutinize the impact of these parameters on combustion performance of a hybrid rocket motor and to investigate the flow physics within them. The fuel used in their experiment was PMMA (Polymethyl Methacrylate) and gaseous oxygen as oxidizer. They have utilized diverse diagnostic techniques, such as high-speed particle image velocimetry and OH\* chemiluminescence imaging, to measure the velocity and temperature fields as well as the reaction zones within the chambers. The experimental outcomes indicate that the pre-combustion chamber had a substantial influence on combustion efficiency, while the post-combustion chamber had a lesser impact. Specifically, the pre-chamber facilitated better mixing of fuel and oxidizer, leading to higher combustion efficiency. It was also observed that the flow structures within the chambers played a pivotal role in determining combustion efficiency.

Arnold<sup>18</sup>, *et al.* studied the effect of prototyping of hybrid fuel grain with fabricated swirling pattern. The authors basically used 3-D printed and casted grains of acrylic and paraffin wax for the experimental purposes. These solid fuel grains either had a projecting vane tabulator centre port or a star-swirl centre port design. Given the complexity of these geometries, they used SolidWorks CAD software to do the post-burn regression rate analysis for the star-swirl geometry to match a computer model with the real burn profile. They noticed regression rate enhancements of more than 270 % in samples of 1/2-tpi acrylic star-swirl. Additionally, a regression rate increase of over 70 % was seen by them when a printed 1/4-tpi tabulator insert was added to cast paraffin that included with 20% aluminium. They reported that energetic additions could be used while retaining swirl-inducing geometry.

Gaurav<sup>19</sup>, *et al.* worked on enhancing the performance with using metal additives in hybrid fuel grain. They used PTFE with aluminium powder to enhance the regression rate and combustion efficiency along with EVA to improve the mechanical properties of the grain. They stated in results that the reactivity of the aluminium enhanced with the use PTFE and it also increased the regression rate with magnitude of 400 %.

After reviewing these papers and going through the various methods utilized to improve the performance of hybrid rocket, it was understood that by changing the grain port configuration would be an alternative and better methods to enhance the performance without using any innovative injection technique. The paper deals about determining and analyzing the regression rate and other performance parameters such as thrust, combustion efficiency etc. by changing the axial alignment of port at multiple axial locations. Apart from it, axial regression rate trend was also analyzed.

## 2. EXPERIMENTAL SETUP AND TEST PROCEDURE

The experimental setup and methodology for ongoing study is described in following subsections.

### 2.1 Experimental Setup

The schematic diagram of the experimental setup is shown in Fig.1. In this study oxidizer cylinders were kept on the weighing balance to get the mass flow rate for particular test by knowing the mass loss of oxygen for the given time of testing. The least count of the weighing machine was 1 gram and maximum weight it can measure was up to 150 kg. Gaseous oxygen was used as an oxidizer in the experiment due to its ease of availability and less hazardous. The volume of cylinder was 47 ltr and made up of steel alloy. The valves used to control the flow and pressure throughout the feed line were the ball valve, dome valve, and solenoid valve. There was a solenoid valve just in front of the motor not more than half a meter away from it so after switching off the oxidizer supply through the dome valve so the feed line must not have much amount of oxidizer left inside since it could start combustion in case if any type of failure occurs in the feed line system. The oxidizer flow rate was maintained at about 30 g/sec at 25 Bar injection pressure.

The sequential timer was used which had the least count of 0.01 sec for controlling the DC power supply to the igniter for 3.90 sec to start the combustion process inside the combustion chamber of HRM and after that DC power was used to supply the current to the solenoid valve to open oxidizer supply for a particular time with respective channels of sequential timer. The 12 V DC power supply was used since the fluctuating current can alter the temperature which would be required for the ignition of the propellant bead.

A data acquisition system (DAQ) was used to measure the pressure fluctuations inside the combustion chamber through a pressure transducer and force exerted during a static firing test on the load cell. The pressure transducer which was used to measure combustion chamber pressure had an upper limit of 50 Bar. The igniter bead was made up of solid composite propellant having weight of 1g and nichrome wire was passed through the bead to conduct current and glow which would increase the temperature inside the bead and leads to the ignition of propellant as well as the combustion process inside the combustor of the hybrid rocket. The major instruments used for the measuring various parameters during the experimentations were piezo resistive pressure transducer, S-type load cell, National instruments data acquisition system, weighing balance, and X-ray machine that were used for getting the burnt profile analysis.

To avoid the fluctuation of the cylinder mass during the mass flow rate of the oxidizer measurement and to get flow rate more accurately with minimum error, the mass flow rate of the oxidizer was obtained before conducting the actual combustion experiments. The oxidizer was made to flow through the rocket motor with the higher time of 10 sec with other parameters maintaining the same as the actual experiment, but no combustion initiated. Due to higher mass loss of oxidizer in a higher time of 10 sec, the errors due to fluctuations of

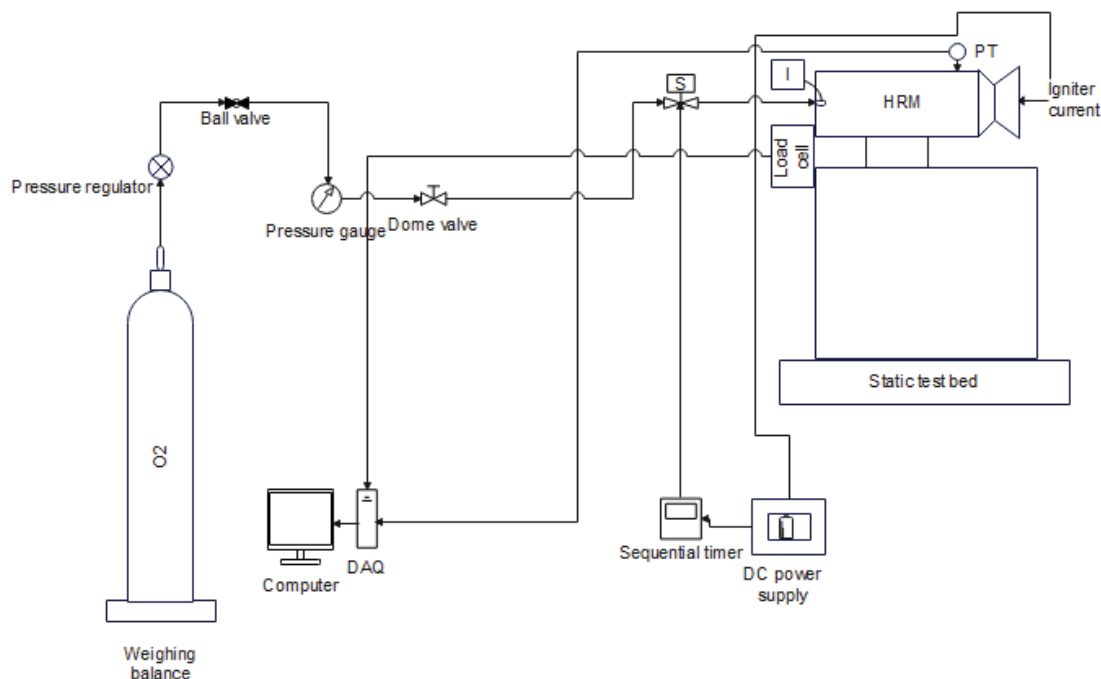


Figure 1. Experimental setup diagram.

weighing balance in the measurement of oxidizer mass flow rate is minimum.

A normal grain with axial port was experimented with and without any configurations of pre or post-combustion chamber setup and the other two types of grain were used with pre and post-combustion chamber setup. In second arrangements of configuration, the grains were cut into 2 equal parts. These two grains were placed into the combustion chamber with the offset port facing opposite to their axis. A gap was provided between them for the smooth flow of the oxidizer from first grain port to the other grain port. The details about is provided in Section 2.3. The gap space was insulated by using a 30 mm initial port fuel grain itself. This gap also works as a post-combustion chamber for the first part of grain and pre-combustion chamber for the upcoming part of the grain. The length of different grains sections installed inside the combustion chamber is provided in Table 1. For sealing the grain inside the motor, a liner was used that was made from PVC-DBP-chalk powder slurry and clay or silicon grease was also used for restricting the burning of grain for the side and end faces.

**Table 1. Length of the grain along axial direction of combustion chamber**

Type of grain	1 <sup>st</sup> part (mm)	2 <sup>nd</sup> part (mm)	3 <sup>rd</sup> part (mm)
Normal port	185	NA	NA
5 mm offset port	80	25	80
10 mm offset port	80	25	80

## 2.2 Hybrid Rocket Motor

A HRM and its components are made up of mild steel due to its reliable mechanical and thermal properties. The HRM combustion chamber had a circular cross-section of diameter

50 mm and a length of 185mm. The showerhead type of injector was made up of mild steel plate. It had 7 holes at a PCD of 15mm. The converging-diverging nozzle is also built from mild steel with graphite layering on the inner surface of the nozzle with a throat diameter of 10mm. The HRM setup used for the present study is shown in Fig. 2.

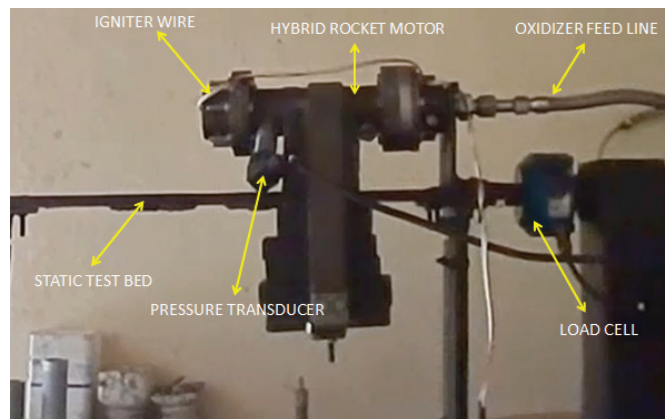


Figure 2. Hybrid rocket motor setup.

## 2.3 Fuel Grain Preparation

The grain used in this experiment had four different port configurations; the first one had a normal port or central port diameter of 15 mm, the second grain of 5 mm offset port from the center with a port diameter of 15 mm, the third type of grain of 10 mm offset port from the center with diameter of 15 mm and the last one had a central port of diameter 30 mm. All these types of grains had the same composition PVC-DBP in the same proportion.

The grain was made up of powdered PVC and liquid DBP taken in 50:50 proportions. All the preparation process starting from weighing, mixing, and casting process was done in a dehumidified conditions. The powdered PVC act as a



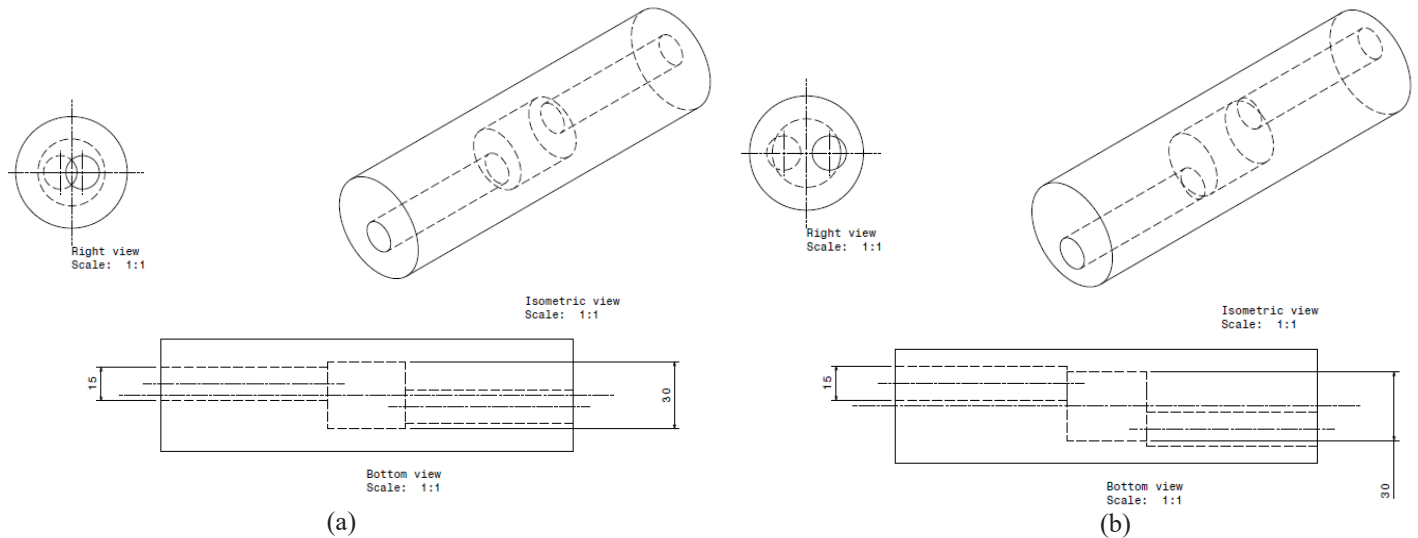


Figure 3. Different port configurations: (a) 5 mm offset port configuration, and (b) 10 mm offset port configuration.

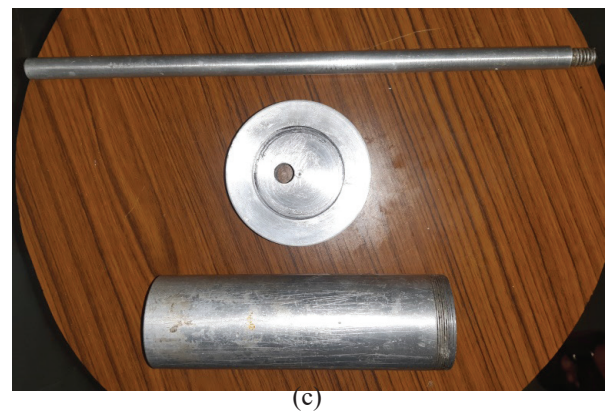
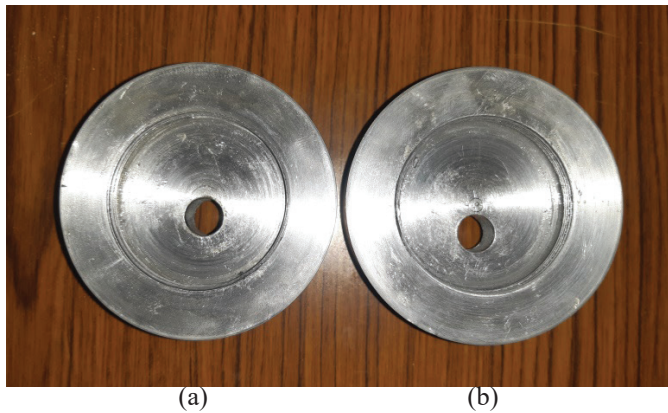


Figure 4. Types of base, mould, and mandrel used: (a) 5mm offset base, (b) 10 mm offset base, and (c) Mandrel, base and mould (up to down respectively).

fuel and liquid DBP acts as the plasticizer. It was utilized to enhance the plastic properties of the grain. It is also known as an energetic plasticizer; the reason behind using it was low cost and easy availability. The homogeneous slurry mixture was obtained through proper blending through a mechanical stirrer at 300RPM for 30 minutes and after that, it was transferred into the mould and mandrel made up of Aluminum metal then followed by a curing process via keeping it in oven for 5 hrs at 120 °C. After that oven was switched off and mould-mandrel was left to cool down inside the oven. The grains were extracted after the curing process for the offset port and central port respectively. The schematic diagrams of the whole grain setup for 5mm offset and 10 mm offset grains used for the study are shown in Fig. 3. The base, mould and mandrel used in this study are shown in Fig. 4.

### 3. RESULTS AND DISCUSSION

#### 3.1 Pressure Analysis

The pressure data were recorded using a piezoresistive pressure transducer which gives voltage fluctuation samples with a sampling rate of 1 kHz during combustion. The data was acquired using the NI DAQ system into the computer. The acquired data that is in the form of voltage was then changed

through a calibrated equation of pressure in the bar and then it was plotted. The signals were rectified in MATLAB software to eliminate noise of the electrical signals that also exist with it and plotted in the same software. The obtained graphs for each types grain configuration is shown in Fig. 5. In Fig. 5, the yellow curve is showing the pressure change inside the combustion chamber for the testing of the central-normal port of 15 mm, and the average chamber pressure was 6.65 Bar. The blue and orange curve is showing the pressure build-up inside the combustion chamber of the same HRM due to the 15mm port grain of 5 mm offset and 10 mm offset respectively.

The average pressure build-up for 5 mm offset grain was 7.28 Bar. The graph shows that at the start of testing the pressure increases a bit and after that stays constant for a while since when the firing started there was obstruction due to the port of the second part in the radially opposite direction so the pressure rose after that oxidizer found the way through the port of second part which shows the constant part and when regression of fuel leads to increase the port area due to which decrease in chamber pressure was observed. The average pressure build-up for 10 mm offset port grain was 8.23 Bar. The combustion chamber pressure of the 10 mm offset grain was more than 5 mm offset port grain since there were two

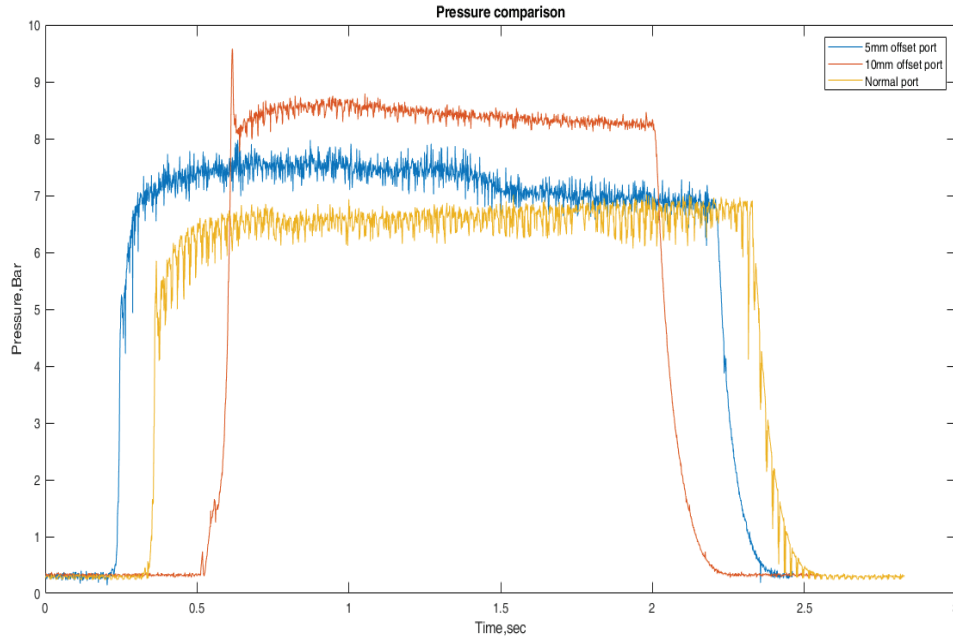


Figure 5. Pressure comparisons for different port grains.

obstructions for the fuel-oxidizer flow mixture, the first one due to the 30 mm normal port grain radial wall and the second one due to the port of second part of the grain in the radially opposite direction that enhances mixing and heat transfer to the grain. It is expected to enhance regression rate and hence the pressure time graph. The curve of 10 mm offset follows the similar path which was observed in 5 mm offset grain. The burn time interval for normal and 5 mm offset port experimentation was 2 sec, while for the 10 mm offset case was 1.5 sec. It was for the safety reasons of the experimentations.

### 3.2 Combustion Efficiency Comparison

The combustion efficiency shows the energy induced within the combustion chamber due to combustion of propellant with respect to the highest energy that could be generated on that particular oxidizer to fuel ratio and even it shows how efficiently the propellant combusted inside the chamber. In this study the combustion efficiency calculated through the ratio of the experimental characteristic velocity ( $C_{exp}^*$ ) to the theoretical characteristic velocity ( $C_{the}^*$ ). The theoretical characteristic jet velocity was calculated through the NASA chemical equilibrium analysis software by assigning proper parameters shown in Table 2.

Table 2. Properties of chemicals used in this study

Ingredients of propellants	Chemical formula	Heat of formation (KJ/mol)
PVC	$C_{2000}H_{3000}Cl_{1000}$	0.69
DBP	$C_{16}H_{22}O_4$	-778

To calculate the experimental characteristic velocity ( $C_{exp}^*$ ) the formula taken from the Sutton and Biblarz<sup>1</sup> which was

$$C_{exp}^* = \frac{P_c A_t}{(\dot{m}_f + \dot{m}_{ox})} \quad (1)$$

$$\eta_{\%} = \left[ \frac{C_{exp}^*}{C_{the}^*} \right] 100 \quad (2)$$

Here in Eqn. (1) and (2), the variables used had their separate meaning like " $P_c$ " denoted the average combustion chamber pressure for a particular testing, " $A_t$ " dictated about the area of nozzle throat and " $\dot{m}_f$ " also " $\dot{m}_{ox}$ " were mass flow rate of fuel and mass flow rate of oxidizer for a particular testing. After using the Eqn. (1) and (2) the combustion efficiency obtained are given in Table 3.

Table 3. Combustion efficiency with respect to grain used in HRM

Type of grain	Pressure build-up (Bar)	O/F ratio	Combustion efficiency (%)
Normal port	6.65	2.46	56.28
5 mm offset port	7.28	1.69	78.67
10 mm offset port	8.12	1.50	80.05

The combustion efficiency ( $\eta_{\%}$ ) of normal port grain during testing in HRM was 56.28 % and for the testing of 10 mm offset grain was 80.05 % at the O/F ratio of 1.50 but for the 5 mm offset port grain it was 78.67 % at O/F ratio of 1.69. The reason for getting higher combustion efficiency in the offset grains was the pre and post combustion chamber setup through central larger port grain (30 mm $\phi$ ). The fuel and oxidizer mixture after reaching larger port area got re-circulated and that enhances mixing. The creation of recirculation zone also helped in the increased residence time, thus the propellant mixture got more time for proper combustion of fuel particles

inside the combustion chamber. The combustion efficiency of 10mm offset grain was more than the 5 mm offset grain due to the relatively enhanced mixing compared to the 5 mm offset grain case.

### 3.3 Regression Rate Comparison

The regression rate calculation was done through the change in weight prior to and after the test firing. In this experiment, regression rate was calculated through the interrupted test method which was proposed by Kumar and Ramakrishna<sup>20</sup>. The port area of grain ( $A_p$ ) was calculated through Eqn. (6) which was taken from Karabeyoglu<sup>21</sup>, *et al.*. In the equations given below every notation have proper meaning, in which “ $d_f$ ” is meant to be the final diameter of port after particular static firing, “ $m_f$ ” meant to be mass fuel burned during particular testing, “ $\rho_f$ ” meant to be density of fuel grain, “ $L_g$ ” meant to be length of the grain, “ $d_i$ ” meant to be initial diameter of grain port before particular firing, “ $t_b$ ” meant to be particular test firing time, “ $\dot{r}$ ” meant to be regression rate for that test firing, “ $G_{ox}$ ” meant to be oxidizer mass flux and “ $\dot{m}_{ox}$ ” stated about mass flow rate of oxidizer.

$$d_f^2 = \frac{4m_f}{\pi\rho_f L_g} + d_i^2 \quad (3)$$

$$\dot{r} = \frac{d_f - d_i}{2t_b} \quad (4)$$

$$G_{ox} = \frac{\dot{m}_{ox}}{A_p} \quad (5)$$

$$A_p = \frac{\pi}{4} \left( \frac{d_f + d_i}{2} \right)^2 \quad (6)$$

After calculation of regression rate through these equations, the obtained data was plotted on graph with respect to mass flux of oxidizer ( $G_{ox}$ ) as shown in Fig. 6.

In the plotted graph which is shown in Fig. 6, the regression rate was calculated through the weight difference method. In the upcoming Eqn. (7), “a” stands for empirical constant and “n” stands for oxidizer flux exponent.

$$\dot{r} = a(G_{ox})^n \quad (7)$$

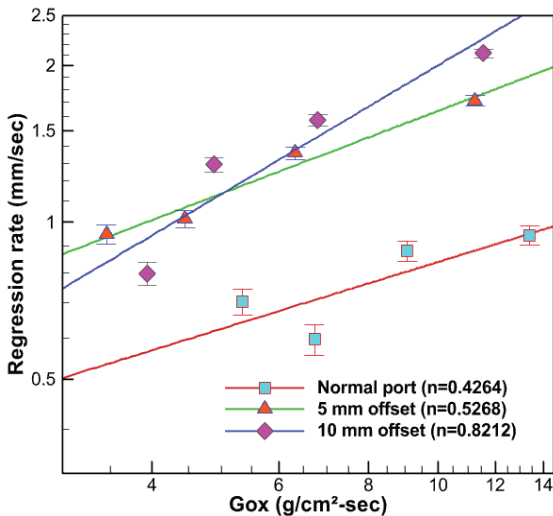


Figure 6. Regression rate vs oxidizer mass flux.

The regression rate of normal port was shown through sky blue boxes on the particular oxidizer mass flux ( $G_{ox}$ ) and red line related to normal port showing power curve of regression rate, similarly orange triangles and pink squares dictating about the regression rate of 5 mm offset and 10 mm offset port grains, respectively.

The maximum regression rate of the normal tubular port grain was 0.94 mm/sec at  $G_{ox}$  of 13.37 g/cm²-sec. For the 5 mm offset port grain, the maximum regression rate was 1.6 mm/sec at  $G_{ox}$  of 11.25 g/cm²-sec and for the 10 mm offset port grain it was 2.1 mm/sec at  $G_{ox}$  of 11.5 g/cm²-sec. It was observed that regression rate of offset port grains was more than the normal port configuration since the use of 30 mm diameter normal port grain configuration worked as a pre and post combustion chamber setup which helped in creating re-circulation zones. These recirculation zones enhanced the mixing and heat transfer to the fuel grain due to increased residence time. These heat transfer phenomenon is more for 10 mm offset grain than 5 mm offset grain, and hence 10 mm offset grain gave higher regression rate compared to normal and 5 mm offset grain. Also, the fuel mixed oxidizer particles coming through the first part of the grain when they reach to the larger port area, the particles also start to strike with the web thickness of the third part of the grain. Again, after colliding from the third part the combustible gases move towards the web thickness part of the first part. The gases moving inside that void space also carrying heat energy due to combustion, so it became easier for the fuel to pyrolyze. The mass flux exponent (n) of normal port grain was 0.43 which indicates decrease in regression rate with increase in oxidizer mass flux. In other motors with a regression rate exponent (n) greater than 0.5, the oxidizer-to-fuel (O/F) ratio increases as the burn time progresses. This indicates that the decrease in regression rate becomes more significant compared to the increase in the burning surface area. In order to get the confidence on the experimental data, a minimum of three repeated experiments were performed and similar results were observed as given in the Fig. 6.

The error has been obtained using the fractional uncertainty method given by Taylor<sup>22</sup>. The maximum uncertainty error obtained for regression rate, oxidizer mass flux and mass flux exponent were 3.64 %, 7.42 % and 8.57 % respectively. The maximum uncertainty error for combustion efficiency was 7.82 %.

As it is observed from the Fig. 6 that the use of 5 mm and 10 mm offset gives a significant improvement in the regression rate. Thus, an attempt was also made to compare with the other existing methods such as protrusion, swirl injection which enhances the regression rate. The care is taken here while comparing that the fuel used by them are also of the same non-liquefying fuel, as it is known that the regression rate behaves differently for liquefying and non-liquefying fuel as reported by Dinesh<sup>23</sup>, *et al.* The comparison graph is shown in Fig. 7. Here, the comparison is made with the protrusion method and swirl injection method with 10 mm offset grain regression rate. In the Fig. 7, the green curve shows the results of the investigation conducted by Dinesh<sup>8</sup>, *et al.* with use of protrusion having the similar size of the motor and the fuel grain. The investigation was performed with non-liquefying fuel which was PVC-DBP



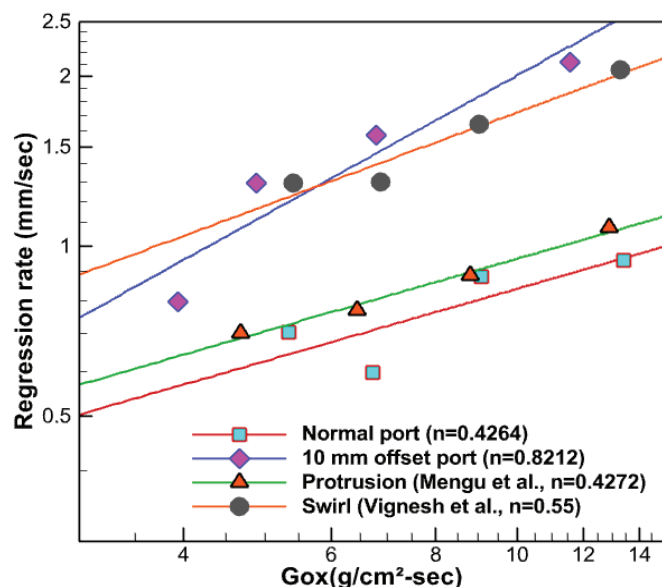


Figure 7. Comparison of 10 mm Offset port regression rate with protrusion<sup>8</sup> and swirl injector methods<sup>11</sup>.

based grain with gaseous oxygen as the oxidizer. The orange curve with black circle was showing the experimentation done by Vignesh<sup>11</sup>, *et al.* on effects of multi-location swirl on the regression rate of hybrid rocket motor. The curve was taken for the same motor and conventional tubular port grain of PVC-DBP grain. The results shown here is with the single swirl injection system. It is observed that the offset grain gives slightly better regression rate even with the swirl injection system.

An attempt was also made to understand the burnt profile of the test fired grain. For this, X-Ray of the burnt grain was taken for the 5 mm offset and 10 mm offset grain. The X-ray images of the grains after combustion are shown in Fig. 8. It can be seen that the erosion of fuel has taken place in both the grain due to the impinging of the oxidizer flow particles over the second grain surface. Also since the flow has to pass through the offset passage, the residence time of the

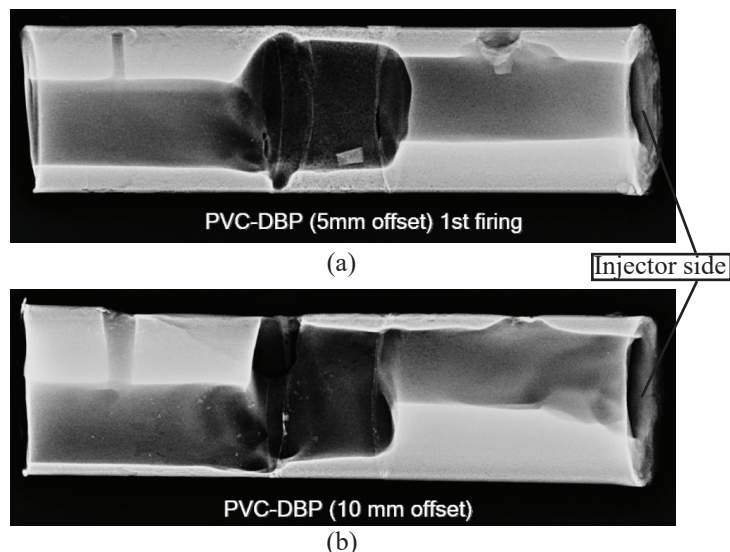


Figure 8. Grains after combustion, (a) 5 mm offset grain after combustion, (b) 10 mm offset grain after combustion.

burnt mixture has increased in the mid-section along with the recirculation zone and thus, maximum erosion of fuel has taken place for both the grain. It can be seen from Fig. 8(a) that the burnt thickness shows an increasing trend in first section of the grain from the injector end to the downstream side. It is due to the increasing mass flux of oxidizer. In the second section of the grain, regression rate or burnt thickness is nearly constant. In Fig. 8(b), the burnt profile has moved towards the offset side, it is due to the offset position with respect to the injector and thus the flow tries to move outwards towards the offset and similarly burning is also seen in that direction. After this the flow turns towards the central axis and combustion also takes place in the similar fashion as seen from the burnt profile. The burnt profile of the second grain section is nearly uniform from mid-section to the end section. In both the offset grains, the burnt profile was nearly uniform in the second section; it is mainly due to the increased total mass flux in the downstream that maintains a constant regression rate along the length.

### 3.4 Force and Volumetric Efficiency Analysis of the Various Port Configurations

Further study was also done to measure the thrust produced due to the change in the grain configuration. A load cell was used to measure the axial force acting due to the static test firing. The load cell works on the concept of Wheatstone bridge resistance arrangement. The load cell transmits force into resistance which was further calibrated in the SI unit. The obtained data was plotted in MATLAB software and further cleaned in signal processing for reduction of noise due to electrical signal. It is shown in Fig. 9. In the graph, blue curve shows the average force generated in the normal port grain static test firing which was around an average of 46.7 N. The orange curve shows the average force generated during the firing of the 5 mm offset port grain which was calculated as 53.4 N and the yellow curve shows the force generated during the firing of the 10mm offset port grain which was observed as 72.3 N. The force generated in both of the offset port grains was higher than the normal port grain since the pressure build-up inside the combustion chamber was more. For a particular flow passing through the 10 mm diameter throat C-D nozzle, the effective jet velocity would be higher for the one coming from a higher pressure region as the force is directly proportional to exhaust jet velocity so it was even expected the force generation in the 10 mm port grain would be higher.

In the graph, blue curve shows the average force generated in the normal port grain static test firing which was around an average of 46.7 N. The orange curve shows the average force generated during the firing of the 5 mm offset port grain which was calculated as 53.4 N and the yellow curve shows the force generated during the firing of the 10mm offset port grain which was observed as 72.3 N. The force generated in both of the offset port grains was higher than the normal port grain since the pressure build-up inside the combustion chamber was more. For a particular flow passing through the 10 mm diameter throat C-D nozzle, the effective jet velocity would be higher for the one coming from a higher pressure region as the force is directly proportional to exhaust jet velocity so it was even expected the force generation in the 10 mm port

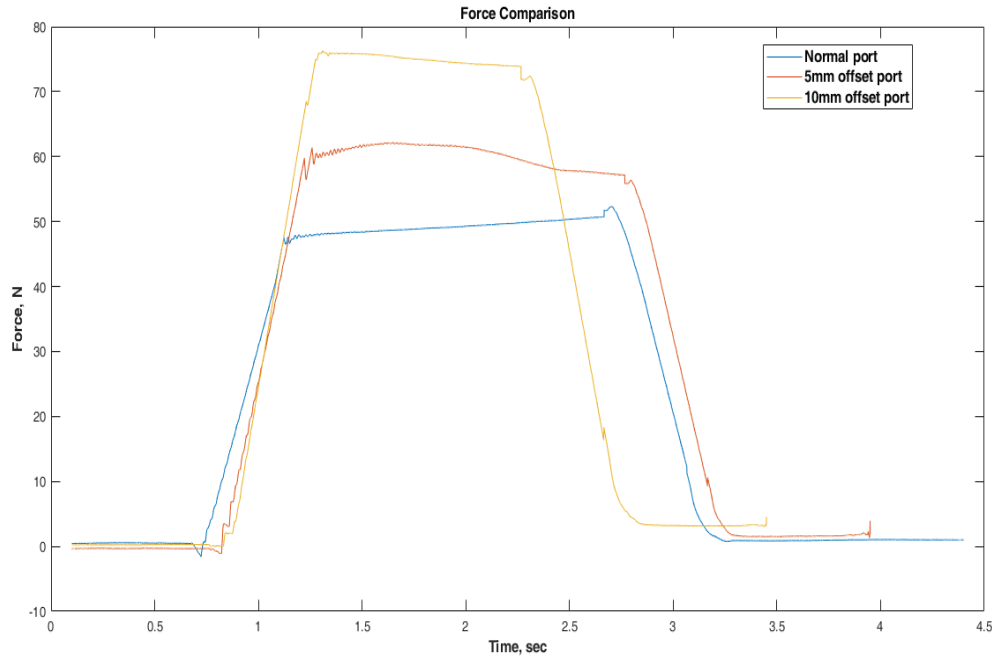


Figure 9. Force comparisons of different port grains.

grain would be higher. The Isp (specific impulse) obtained were in the range of 850-1150 Ns/kg. These values are small compared to the actual values; it might be due to the lower combustion efficiency as discussed earlier in Section 3.2. The volumetric efficiency was calculated through the ratio of total volume occupied by the grain with respect to the total volume available in the combustion chamber. The volumetric efficiency came out to be 72.6 % for both of the grain which was quite low in the comparison of the conventional tubular port grain which had the volumetric efficiency of 91 %. It is mainly due to the cavity or space provided in between the two grains. It is to be noted that in most of the hybrid rocket system uses pre and post combustion chamber for the improvement of performance parameters. Here, having cavity is still better than having pre and post combustion chamber as it has given significant improvement in the regression rate and thrust. The main objective of providing cavity here is to provide the space for the passage of oxidizer from first chamber to the next fuel grain chamber. It could be further optimized by providing suitable path to enter the oxidizer from first chamber to another in a helical way without leaving any cavity, which is expected to improve regression rate as well as volumetric efficiency.

#### 4. CONCLUSIONS

In the present study, the performance parameters were analysed by using the grains of offset port alignment from the axial position. The offset ports were alternatively placed in the combustion chamber. It was further compared with the normal axial port of 15 mm. The pressures build up inside the combustion chamber for offset port grains were higher than that of normal port grain case. It was observed that the pressure was 1 to 2 Bar more than the offset port grains case. The force exerted by the HRM for offset port grain was 10 to 25 N higher than the force generated in normal port grain static test firing. The regression rate for the offset port grains at a given oxidizer

mass flux is higher than the regression rate observed with a normal port grain case. The combustion efficiency for the offset port grains was also 5 to 6 percent higher than the normal port grains case.

#### REFERENCES

1. Sutton, G.P. & Biblarz, O. Rocket propulsion elements. John Wiley & Sons, England, 2001. 580 p.
2. Ramamurthi K, Rocket Propulsion, Trinity Press of Laxmi Publications Private Limited, India, 2016. 229 p.
3. George, P.; Krishnan, S.; Varkey, P.M.; Ravindran, M. & Ramachandran, L. Fuel regression rate in HTPB/gaseous oxygen hybrid motors. *J. Propul. Power.*, 2001, **17**(1), 35–42.  
doi: 10.2514/2.5704
4. Chiaverini, M.J.; Serin, N.; Johnson, D.K.; Lu, Y.C.; Kuo, K.K. & Risha, G.A. Regression rate behaviour of hybrid rocket solid fuels. *J. Propul. Power.* 2000, **16** (4), 125–132.  
doi: 10.2514/2.5541
5. Frederick, R.A.; Whitehead, J.J.; Knox, L.R. & Moser, M.D. Regression rates study of mixed hybrid propellants. *J. Propul. Power.* 2007, **23**(1), 175–180.  
doi: 10.2514/1.14327
6. Lee, C.; Na, Y.; Lee, J.W. & Byun, Y.H. Effect of induced swirl flow on regression rate of hybrid rocket fuel by helical grain configuration. *Aero. Sci. Technol.* 2007, **11**, 68–76.  
doi: 10.1016/j.ast.2006.07.006
7. Kumar, R. & Ramakrishna, P.A. Effect of protrusion in the enhancement of regression rate in hybrid rockets. *Aero. Sci. Technol.*, 2014, **39**, 169–178.  
doi: 10.1016/j.ast.2014.09.001
8. Dinesh, M. & Kumar, R. Utility of multi-protrusion as performance enhancer in hybrid rocket motor. *J. Propul.*



- Power.*, 2019, **35**(5), 1-13.  
doi: 10.2514/1.B37491
9. Dinesh, M. & Kumar, R. Experimental studies of protrusion inserted hybrid rocket motor with varying L/D ratio. *J. Spacecr. Rockets.*, 2020, **58**(2), 1-17.  
doi:10.2514/1.A34759
  10. Kumar, R. & Ramakrishna, P.A. Enhancement of hybrid fuel regression rate using a bluff body. *J. Propul. Power.* 2014, **30**(4), 909-16.  
doi: 10.2514/1.B34975
  11. Vignesh, B. & Kumar, R. Effect of multi-location swirl injection on the performance of hybrid rocket motor. *Acta Astronaut.* 2020, **176**(1), 111-23.  
doi: 10.1016/j.actaastro.2020.06.029
  12. Kumar, P. & Kumar, A. Effect of swirl on the regression rate in hybrid rocket motors, *Aero. Sci. Technol.* 2013; **29**, 92-99.  
doi: 10.1016/j.ast.2013.01.011
  13. Tian, H.; Sun, X.; Guo, Y. & Wang, P. Combustion characteristics of hybrid rocket motor with segmented grain. *Aero. Sci. Technol.* 2015, **46**(1), 537-47.  
doi: 10.1016/j.ast.2015.08.009
  14. Sakashi, H.; Saburo, Y.; Kousuke, H. & Takashi, S. Effectiveness of concave-convex surface grain for hybrid rocket combustion. AIAA-2012-4107.  
doi: 10.2514/6.2012-4107
  15. Kearney J. Circumstantially fired combustion port geometry: analysis of hybrid rocket motor solid fuel grain. California State University, Sacramento). (PhD thesis).
  16. Makle, A.; Zaye, A.N.; Abdalla, H. & Senbawi, M. Effect of post-chamber on combustion efficiency in hybrid rocket motors. In International Conference on Aerospace Sciences and Aviation Technology 2003 May 1 (Vol. 10, No. 10<sup>th</sup> International Conference on Aerospace Sciences & Aviation Technology, pp. 253-266). The Military Technical College.  
doi:10.21608/asat.2013.24425
  17. Mechentel, F.S. & Cantwell, B.J. Experimental findings on pre-and post-combustion chamber effects in a laboratory-scale motor. AIAA-2019-4336.  
doi: 10.2514/6.2019-4336
  18. Arnold, D.; Boyer, J.E.; Kuo, K.; Fuller, J.K.; Desain, J. & Curtiss, T.J. Test of hybrid rocket fuel grains with swirl patterns fabricated using rapid prototyping technology. AIAA-2013-4141.  
doi: 10.2514/6.2013-4141
  19. Marothiya, G. & Ramakrishna, P.A. Combustion of Flake Aluminum with PTFE in Solid and Hybrid Rockets. *Nano and Micro-Scale Energetic Materials: Propellants and Explosives.* 2023, **1**, 333-376.  
doi: 10.1002/9783527835348.ch12
  20. Kumar, R. & Ramakrishna, P.A. Issues related to the measurement of regression rate of fast-burning hybrid fuels. *J. Propul. Power.* 2013, **29**(5), 1114-21.  
doi: 10.2514/1.B34757
  21. Karabeyoglu, M.A.; Cantwell, B.J. & Ziliac, G. Development of scalable space-time averaged regression rate expressions for hybrid rockets. *J. Propul. Power.* 2007, **23**(4), 737-47.  
doi: 10.2514/1.19226
  22. Taylor, J.R. "Propagation of Uncertainties," an Introduction to Error Analysis: the Study of Uncertainties in Physical Measurements, University Science Book, Sausalito, California, 1997, pp. 45-79.
  23. Dinesh, M.; Rajput, S.S. & Kumar, R. Protrusion effect on the performance of hybrid rocket with liquefying and non-liquefying fuels. *Acta Astronaut.* 2021, **178**, 536-47.  
doi:10.1016/j.actaastro.2020.09.039

#### ACKNOWLEDGEMENTS

The authors express their sincere gratitude to the staffs and colleagues of the Space Engineering and Rocketry Department, BIT Mesra for providing the lab facility to carry out this research work.

#### CONTRIBUTORS

**Mr Gyandeep** is perusing his Master of Technology in the Department of Space Engineering and Rocketry, Birla Institute of Technology, Mesra, Ranchi. He studied the effect of change in port alignment in hybrid rocket motor on its performance parameters.

His contributions in the current study include: Investigation and writing-original draft preparation.

**Dr Rajiv Kumar** obtained his PhD degree from the Aerospace Engineering Department of IIT Madras in 2014. Currently, he is working as an Assistant Professor in the Space Engineering and Rocketry Department. He worked on Propellant characterization and its uses in solid rocket motor, effect of various parameters such as injectors, protrusion, additives etc. on hybrid rocket performance, Liquid rocket test firing, Atomization and Spray characterization.

His contribution in the current study include: Conceptualization, writing, reviewing and editing.